RAMAN PROBING OF PHONONS AND INTERFACES IN SEMICONDUCTOR SUPERLATTICES

M. Klein, C. Colvard, R. Fischer, H . Morkoç

JOURNAL DE PHYSIQUE
Colloque C5, supplément au n°4, Tome 45, avril 1984

RAMAN PROBING OF PHONONS AND INTERFACES IN SEMICONDUCTOR SUPERLATTICES

M.V. Klein[1,2,3], C. Colvard[1,2], R. Fischer[3,4] and H. Morkoç[3,4]

Department of Physics[1], Materials Research Laboratory[2], Coordinated Science Laboratory[3] and Department of Electrical Engineering[4], University of Illinois at Urbana-Champaign, Urbana, IL 61801, U.S.A.

Résumé - Dans cet article, nous présentons des mesures de diffusion Raman dans un grand nombre de superréseaux. Les fréquences observées sont en accord avec un modèle élastique décrivant un matériel construit avec des couches alternées. Un modèle continu décrivant les intensités observées par diffusion Raman s'applique bien dans des conditions non-résonnantes.

Abstract - Raman measurements on a large number of GaAs-$Al_xGa_{1-x}As$ superlattices are presented. The observed frequencies are in agreement with the model of a layered elastic continuum. A continuum model for the Raman intensities seems valid for the case of nonresonant excitation.

Many properties of semiconductor superlattices (SL) and multiple quantum well (MQW) heterostructures have now been studied. Interest has grown in parallel with the ability to grow good quality samples with sharp interfaces. Much effort has lead to good understanding of the two-dimensional effects caused by confinement of electrons in the quantum wells. Only when the barriers are thin does three-dimensional electron behavior begin. Much less experimental work has been reported on phonons in superlattices. The most dramatic effects result from zone folding, and this paper will concentrate on them.

Raman studies of folded acoustic phonons have now been reported by several groups /1-4/. Unlike the case of electronic energy levels, which show confinement, these phonon modes show coherence across many layers. They therefore provide information about layer-to-layer uniformity that complements that from probes of confined electron states. The SL periodicity shrinks the bulk Brillouin zone into a mini-zone, folds the phonon dispersion curves, and opens small gaps due to Bragg reflection. We have used Raman scattering to study these folded phonons in a number of SL samples grown by molecular beam epitaxy (MBE) and present here some of the results.

The samples have periods between 25 and 200 Å and consist of alternate layers of GaAs and $Al_xGa_{1-x}As$ with various x values grown on [001] oriented GaAs substrates. Most of the Raman data presented here were taken at room temperature in a Brewster angle, backscattering geometry. For incident light polarized along [100] and scattered light polarized along [010], denoted (x,y), the Raman selection rules allow only modes of B_2 symmetry to be observed if the crystal has D_{2d} symmetry. For the (x,x) geometry only A_1 modes are allowed.

The [001] dispersion for an LA phonon shown in the inset of Fig. 1 demonstrates the effect of the layering on longitudinal modes in a SL with 42 Å GaAs and 8 Å $Al_{0.3}Ga_{0.7}As$ per period. Gaps appear at the zone center and edge, whereas at low frequencies the remaining dispersion is essentially linear. This

curve was calculated using an elastic continuum model for acoustic phonons, i.e. a Kronig-Penney model for phonons. /5,2,4/ The crosses represent the lowest three orders of folded phonons that can conserve momentum while scattering light of 5145 Å wavelength. The phonon wave-vector is nearly normal to the layers and is given by

$$q = 4\pi n/\lambda_L, \tag{1}$$

where n is the refractive index at wavelength λ_L. We assume n to be the same as that in an alloy with the same average Al content. The calculations show that for frequencies away from the small gaps the folded phonons occur as doublets with frequencies

$$\omega = (q_m \pm q)\ \bar{v}_{SL} \tag{2a}$$

where m is an integer and

$$q_m = 2\pi m/d, \tag{2b}$$

and where

$$\frac{1}{\bar{v}_{SL}} \approx \left\langle \frac{1}{v_{bulk}} \right\rangle . \tag{3}$$

Such results are obtained by neglecting the perturbation caused by the SL on zero-order plane waves propagating with velocity $\bar{v}_{SL}$.

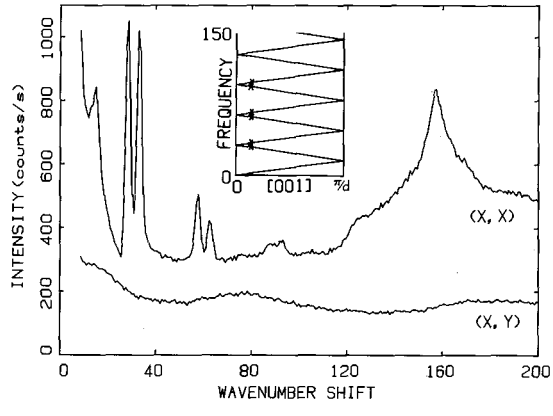

Figure 1 — Raman spectrum at λ_L = 5145 Å of a SL with 100 periods of 42 Å GaAs–8 Å $Al_{.3}Ga_{.7}As$ showing folding up to $\bar{m} = 3$ and a 2 TA structure. Insert indicates q_z of folded doublets.

The Raman spectrum in Fig. 1 shows data taken from such a SL using 5145 Å laser light. Apparent are the doublets corresponding to m = 1 to 3 and a 2TA structure whose origin may be partly due to the GaAs substrate. The A_1 component appears in the upper (x,x) curve. The absence of any B_2 scattering in the lower (x,y) curve is due to the effective inversion symmetry of the SL seen by these long-wavelength acoustic modes. /4/ The B_2 part of the spectrum would represent the odd-parity component of the vibrations, and coupling to it would be forbidden for Raman scattering in a lattice with inversion symmetry. The peak at 15 cm^{-1} is related to the zone boundary. Its appearance seems to be a general phenomenon, but it will not be further discussed here.

Figure 2 shows spectra from a sample with 13.9 Å GaAs and 11.6 Å AlAs per period. One again sees the m = 1 longitudinal doublet near 67 cm^{-1} and in addition small peaks near 45 cm^{-1} due to transverse phonons. These latter modes have E-symmetry in the SL, and this is a forbidden geometry for backscattering from a [001] face. However the Brewster angle geometry used here introduces a small z-component of polarization, which may account for their appearance. Disorder may also play a role.

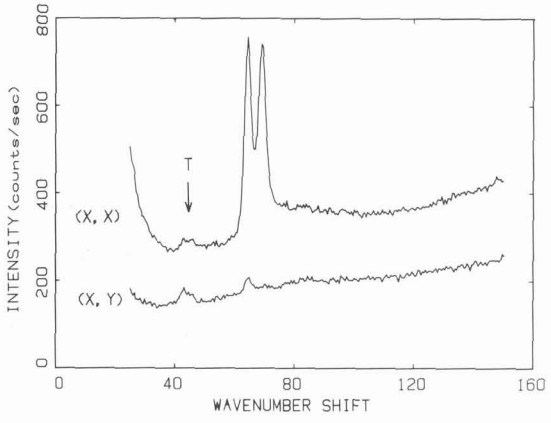

Figure 2 - Raman spectrum of a 13.9 Å GaAs-11.6 Å AlAs SL with λ_L = 5145 Å. E-symmetry transverse phonons are indicated by T.

The sample used for Fig. 2 was also used to determine the phonon dispersion to the extent that the phonon wavevector q_z can be varied by varying λ_L between 4579 Å and 6764 Å. The results are shown in Fig. 3, and are compared with calculations using a linear chain model with 5 monolayers of GaAs and 4 monolayers of AlAs per period. Atomic masses were used, and the single force constant was chosen to provide the correct sound velocity for bulk GaAs. For larger periods this type of model agrees with the elastic continuum model mentioned above. /6/ Note that even with such a small period we are just barely in the region where Bragg reflection causes curvature in the dispersion curves, i.e., partially changes the zero-order running wave into a standing wave.

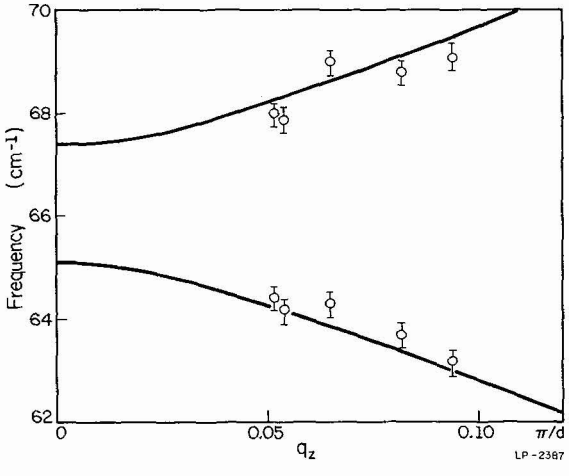

Figure 3 - Folded phonon frequency at various laser wavelengths in a SL with 13.9 Å GaAs-11.6 Å AlAs. Solid curve is a linear chain model calculation.

The results of measurements on a variety of samples are summarized in Fig. 4, where the frequency of the folded phonon doublets is plotted versus d^{-1}. The average sound velocity $\bar{v}_{SL}$ varies with Al content, but the trends are indicated by the shaded regions which are bounded by $q_m v_{GaAs}$ for longitudinal acoustic waves in GaAs and by $q_m v_{AlAs}$, where v_{AlAs} is estimated from v_{GaAs} by simply changing the mass density. In all cases the doublet splitting is close to $2q\bar{v}_{SL}$. The two lower frequency doublets at small d represent transverse modes. Uncertainties in the period d result either from nonuniformity across the face of the sample or from lack of good x-ray data. This plot suggests that Raman scattering can be used to determine the SL period over well-defined small regions of a sample.

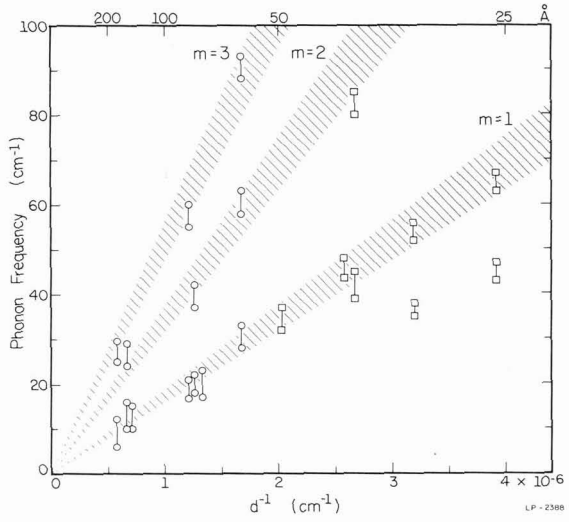

Figure 4 - Observed folded acoustic phonon frequencies vs. inverse SL period. Shaded regions indicate frequencies bounded by bulk sound velocities. Squares indicate samples with AlAs barriers, circles refer to $Al_{.3}Ga_{.7}As$ barriers.

We notice in the plot of Fig. 4 that some samples show both first and third order folding (i.e., m = 1,3) but no second order folding (m = 2). Figure 5 presents data showing this taken on a sample with 41 Å GaAs - 41 Å $Al_{0.3}Ga_{0.7}As$.

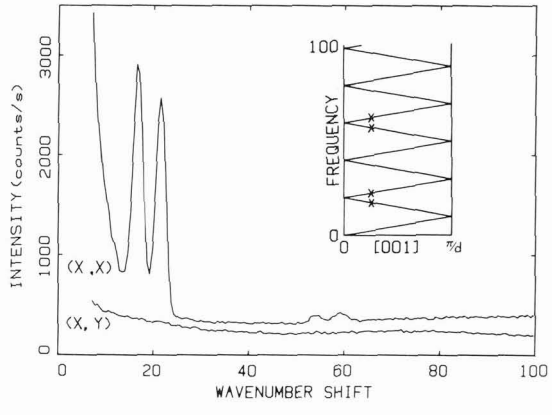

Figure 5 - SL with 41 Å GaAs-41 Å $Al_{.3}Ga_{.7}As$ showing missing second order folding. Data taken with λ_L = 5145 Å.

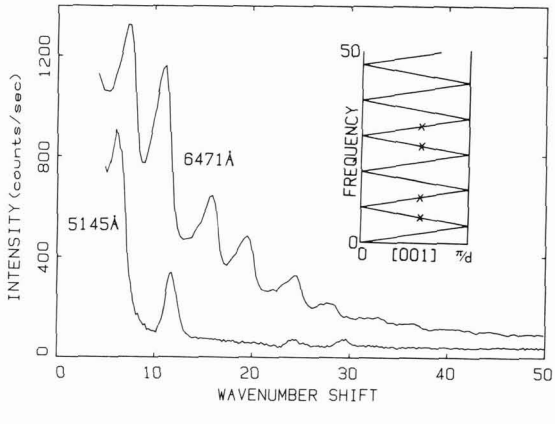

Figure 6 - Raman spectra at two laser wavelengths from an 83 Å GaAs-90 Å $Al_{.3}Ga_{.7}As$ SL in (x,x) geometry. Inset shows q_z for peaks in lower curve.

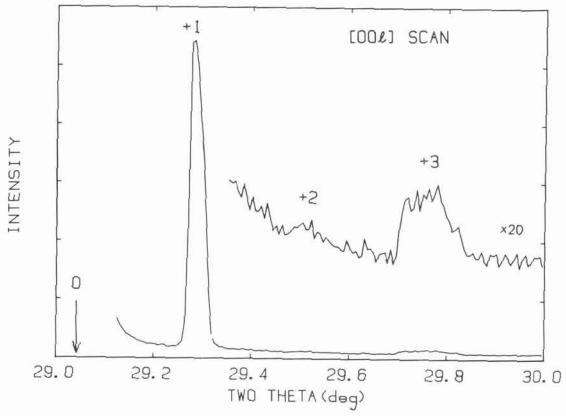

Figure 7 - X-ray data for sample of Fig. 6 showing first three satellite positions.

A second example is shown in Fig. 6, where the lower curve from a 83 Å GaAs-90 Å $Al_{0.3}Ga_{0.7}As$ sample was taken with λ_L = 5145 Å in the (x,x) geometry. The missing m = 2 order can be explained by the theory outlined below, which correlates the intensities of the folded phonons with structural information. The x-ray data shown in Fig. 7 shows almost no m = 2 satellite for the sample of Fig. 6.

We now sketch a continuum model that allows a calculation of the intensity of Raman scattering from folded LA phonons. The smallness of the gaps and the linearity of the calculated dispersion curves suggest that away from the gaps the LA displacement field can be approximated by the plane wave

$$u(z) = u_k e^{ikz} \tag{4}$$

with frequency $\omega = \bar{v}_{SL} k$. For photon energies away from interband resonances, the photoelastic coefficient P(z) should approximately take the form

$$P(z) = \frac{dP}{dx} x(z) , \tag{5}$$

where x(z) is the concentration of Al at depth z in the SL. For an ideal superlattice with abrupt interfaces P(z) will be a square wave, given over one SL period by

$$P(z) = P_a \text{ when } 0 \leq z < d_1 \tag{6a}$$

$$P(z) = P_b \text{ when } d_1 \leq z < d = d_1 + d_2. \tag{6b}$$

By analogy with ordinary Brillouin scattering, we assume that the scattered intensity obeys /7/

$$I(\omega) \propto \langle |\delta\chi_q|^2 \rangle_\omega \tag{7a}$$

where for longitudinal strains $\partial u/\partial z$

$$\delta\chi_q = L^{-1} \int_0^L e^{-iqz} P(z)[\partial u(z)/\partial z]dz, \tag{7b}$$

where L is the normalization depth of the sample. Since P(z) is periodic, we expand in a Fourier series

$$P(z) = \sum_m P_m \exp(iq_m z) \tag{8}$$

and find for the q^{th} component of the optical susceptibility

$$\delta\chi_q = \sum_m P_m \, i(q - q_m) \, u_{q-q_m} . \tag{9}$$

The m = 0 term in (9) describes Brillouin scattering at $\omega = q\bar{v}_{SL}$ with intensity

$$I_{Brill} \propto k_B T |P_0|^2 \tag{10a}$$

where P_0 is the average of P(z) given by

$$P_0 = d^{-1}(d_1 P_a + d_2 P_b). \tag{10b}$$

The $\pm$ m terms in (9) describe Raman scattering from folded phonons at $\omega = |q \mp q_m|\bar{v}_{SL}$ and intensity

$$I_m \propto k_B T \, |P_m|^2 . \tag{10c}$$

Using Eq. (6) to determine P_m we find

$$\frac{I_m}{I_{Brill}} = \frac{(P_a - P_b)^2}{P_0^2} \; \frac{|\sin \pi m d_1/d|}{\pi^2 m^2} . \tag{11}$$

As expected from Fourier analysis of a square-wave when $d_1 = d_2 = 1/2$ d, Eq. (11) gives $I_m = 0$ for m even.

When the laser photon energy is selected to be near the $E_o + \Delta_o$ gap of the sample of Fig. 6, the m = 2 and m = 4 peaks now appear, and the m = 2,3 peaks shift to lower frequency and become asymmetric. Though not yet completely understood, this behavior has several possible explanations. (i) It is no longer possible to define a local photoelastic coefficient P(z) as we did above for the non-resonant case. In resonance one obtains non-local behavior determined by the range of the SL wavefunctions in the individual quantum wells and between the wells. Thus Eq. (11) is no longer valid. (ii) The asymmetric lineshapes are probably due to an anti-resonant coupling between the phonons and a continuum. The latter may be seen in Fig. 6 as a "laser tail." Possible candidates for the continuum include electronic scattering and two-phonon difference processes. In other samples near an electronic resonance we have indications of anti-resonant behavior of both folded phonons obeying wavevector conservation and those from the minizone boundaries.

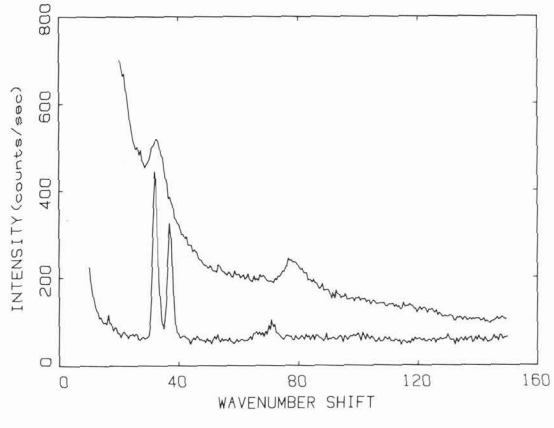

Figure 8 - Raman spectra of two SL's with λ_L = 5145 Å in (x,x) geometry. Upper curve: 12.5 Å GaAs-37.5 Å AlAs. Lower curve: 37.5 Å GaAs-12.5 Å AlAs.

All the Raman results mentioned above were obtained on samples of GaAs alternating with $Al_xGa_{1-x}As$ where the average Al content was less than 50%. Some

samples have been studied with greater amounts of Al, either by using thick AlAs layers or by adding Al to the GaAs layers. In such samples the Raman data are consistently inferior; the phonon doublets are replaced by broad, often indistinct, structures. An example is shown in Fig. 8, where data from two d ≈ 50 Å samples are shown, both grown at a substrate temperature of 600°C. The upper curve refers to a sample with 12.5 Å GaAs and 37.5 Å AlAs, and the lower curve to a sample with 37.5 Å GaAs - 12.5 Å AlAs. No x-ray satellites were found for the former sample. One explanation for the difference between the spectra is an increased layer uniformity and interfacial order caused by the smoothing effect of thicker GaAs layers. /8-9/

In conclusion, we have demonstrated experimentally and theoretically that the Raman spectrum from folded LA phonons contains structural information that correlates well with x-ray diffraction results from (00ℓ) scans. Raman spectra in higher frequency regions are also affected by superlattice formation, but the changes are subtler and less well understood than those of acoustic phonons discussed here.

We thank T. J. Drummond, J. Klem, and T. Henderson for assistance with sample preparation and T. Gant for help with the Raman measurements. X-ray diffraction measurements were made by H. Zabel, D. Gross and S. L. Cooper in the MRL microstructure facility. A. C. Gossard provided several small-period samples. This work was supported by NSF under DMR 82-03523, JSEP under N-00014-79-C-0424 and by AFOSR under F49620-83-K-201.

REFERENCES

1. BARKER, A. S., MERZ, J. L., GOSSARD, A. C., Phys. Rev. B17 (1978) 3181.

2. COLVARD, C., MERLIN, R., KLEIN, M. V., GOSSARD, A. C., Phys. Rev. Lett. 45 (1980) 298.

3. COLVARD, C. MERLIN, R., KLEIN, M. V., GOSSARD, A. C., J. Phys., (Paris) Colloq. 42 (1981) C6-631.

4. SAPRIEL, J., MICHEL, J. C., TOLEDANO, J. C., VACHER, R., KERVAREC, J., REGRENY, A., Phys. Rev. B28 (1983) 2007.

5. RYTOV, S. M., AKUST. Zh. 2 (1956) 71 [Sov. Phys. Acoust. 2 (1956) 68].

6. SAPRIEL, J., DJAFARI-ROUHANI, B., DOBRZYNSKI, L., Surface Science 126 (1983) 197.

7. HAYES, W., LOUDON, R., Scattering of Light by Crystals (Wiley, N.Y., 1978).

8. MILLER, R. C., GOSSARD, A. C., TSANG, W. T., Physica 117B & 118 B (1983) 714.

9. DRUMMOND, T. J., KLEM, J., ARNOLD, D., RISCHER, R., THORNE, R. E., LYONS, W. G., MORKOÇ, H., Appl. Phys. Lett. 42 (1983) 615.